Pulsed Photofission Delayed Gamma Ray Detection for Nuclear Material Identification

2012 NSS/MIC

John Kavouras
Xianfei Wen
Daren R. Norman
Dante R. Nakazawa
Haori Yang

November 2012

Idaho National Laboratory

Pulsed Photofission Delayed Gamma Ray Detection for Nuclear Material Identification

John Kavouras, Xianfei Wen, Daren R. Norman, Dante R. Nakazawa, Haori Yang, *Member, IEEE*

Abstract– **Innovative systems with increased sensitivity and resolution are in great demand to detect diversion and to prevent misuse in support of nuclear materials management for the U.S. fuel cycle. Nuclear fission is the most important multiplicative process involved in non-destructive active interrogation. This process produces the most easily recognizable signature for nuclear materials. High-energy gamma rays can also excite a nucleus and cause fission through a process known as photofission. After photofission reactions, delayed signals are easily distinguishable from the interrogating radiation. Linac-based, advanced inspection techniques utilizing the fission signals after photofission have been extensively studied for homeland security applications. Previous research also showed that a unique delayed gamma ray energy spectrum exists for each fissionable isotope. Isotopic composition measurement methods based on delayed gamma ray spectroscopy will be the primary focus of this work.**

I. Introduction

In photofission reactions, four types of radiation can be used as signature signals for material identification and quantification: prompt photons, prompt neutrons, delayed photons, and delayed neutrons. Although prompt signals are much stronger than the delayed signals, it is difficult to quantify them in practical measurements. There are several reasons they are hard to measure including that they tend to be buried by the more intense probing radiation, detector recovery time, inelastic neutron scattering, and the very short lived activation products. Delayed signals are emitted seconds or even minutes after the photon irradiation making it easier to be distinguished from the interrogating radiation. Linac-based, advanced inspection techniques utilizing the delayed signals after photon induced fission have been extensively studied for homeland security and safeguards applications [1-20]. Previous research also showed that a unique delayed gamma ray energy spectrum exists for each fissionable isotope [6-12, 14,15,17, 19-21]. Isotopic composition measurement methods based on delayed gamma ray spectroscopy will be the primary focus of this project.

The primary focus of this work is to study active interrogation methods based on delayed gamma ray spectroscopy following photon induced fission, for Material Protection, Accounting and Control Technologies (MPACT). Delayed gamma rays have a wide range of half-lives ranging from fractions of a second to many years after the induced fission. Approximately, 6 to 8 of these delayed gamma rays are emitted following each fission process. This is over 100 times more abundant than the yield of delayed neutrons. Delayed gamma ray energy spectrum is unique for each fissionable isotope. Although quite rich and complicated, delayed gamma ray spectra can be measured and analyzed using modern high resolution gamma spectroscopy systems. The relative amplitudes of certain lines vary significantly from one isotope to another. This is a result of the difference in photofission yield distribution of various isotopes. For example, discrimination ratio, measured as the intensity ratio between the 1103 keV Y-97 peak and the 1032 keV Rb-89 peak, were observed to be significantly different between U-235, Pu-239 and U-238 [19,20]. Observations like this can be utilized to measure isotopic composition in nuclear material samples. Previous research has shown that delayed gamma ray spectra emitted by fission products can be measured in seconds or even minutes after the induced fission using high purity germanium (HPGe) detectors [21]. Both the energy information and the temporal behavior based on the half-life of the observed gamma ray peaks can be used to identify and quantify fission products. Using the knowledge on photofission yield distribution of various isotopes and the irradiation and count time intervals, the isotopic composition of the sample can then be deduced.

The intensity of the delayed gamma rays decreases rapidly after the induced fission. Thus, the detection sensitivity can be dramatically increased by performing the measurements shortly after the induced fission reactions. Previous research shows that this can be accomplished using innovative digital electronics [22]. The performance of using photofission techniques for direct measurement of plutonium in spent fuel will be thoroughly investigated in this proposed project.

II. Initial Testing

An initial test was performed at INL. Combinations of various electronics, detectors, and experimental setups were tested and evaluated. The experimental setup is shown in Figure 1. The detector and front-end electronics are positioned in a shielded cavity built with lead and bismuth bricks. This detector and shielding assembly is located out of the linac beam at a low backscattering angle. The detector is pointing at

a sample placed in the beam. The distance between the Bremsstrahlung target and the sample is 40 cm. The distance between the sample and the front end of the detector is 21 to 41 cm depending on the detector used.
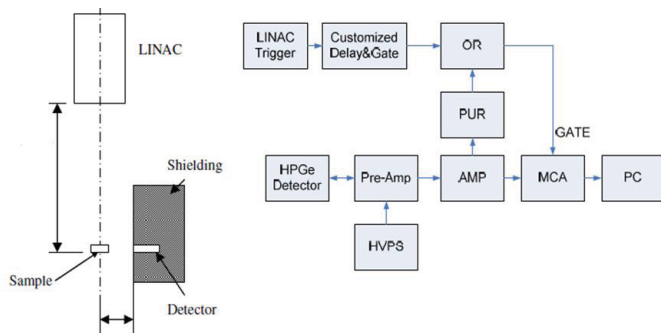

Fig. 1. Experimental setup of the initial testing.

During these measurements, a RF-based S-Band linac provided various pulse rates, beam currents, and beam energies. The maximum pulse rate used for the testing was 125 Hz, with each pulse's duration being about 3.5 micro-seconds. The beam current was adjusted to assess the detectors' performance, with the maximum average beam current of 3.2 micro-amps for the 10 MeV operations.

A. Interlace Mode Measurements

The simplest and most straight-forward way to measure delayed gamma rays after photofission is to use an interlace mode. In this mode, the sample is irradiated for a certain amount of time. Then the linac is turned off and after some delay time the spectrometry measurement starts. This irradiation-counting sequence can be repeated until satisfactory counting results are obtained. A schematic is shown in Fig. 2. The irradiation time, detector recovery or cooling time, and counting time can be chosen to optimize specific nuclide production for various operational configurations. [23]
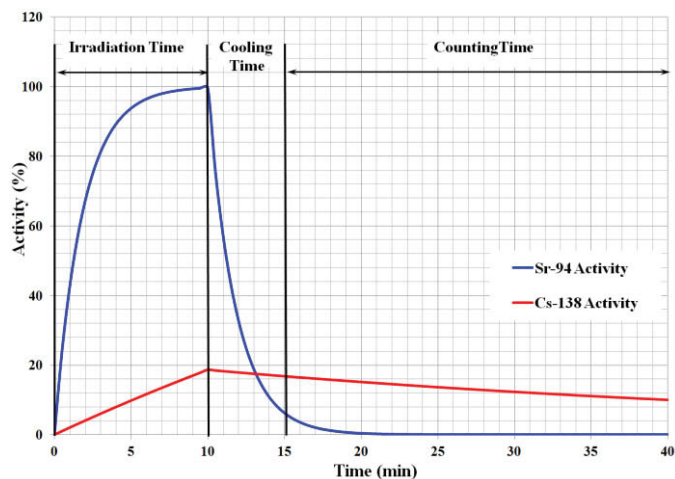

Fig. 2. Schematic of the interlace mode measurement showing the activity of Sr-94 and Cs-138 with a 10 min irradiation and 5 min cooling time

Spectra were measured using this method, with both DU and HEU samples. Full energy peaks from fission products have been observed and identified in these spectra. Although counting in interlace mode is easy to implement, short-lived fission products are hard to identify and quantify based on spectra measured this way. Shorter-lived isotopes die away faster after each linac pulse. Thus, after the irradiation period, the only short-lived isotopes measured were produced at the end of the irradiation. On the other hand, the measured activity of long-lived isotope is the integral activity over the whole irradiation period. As shown in Fig. 3 below, the shorter-lived Sr-94 is less prominent than the longer-lived Cs-138, although Sr-94 has a larger fission yield.
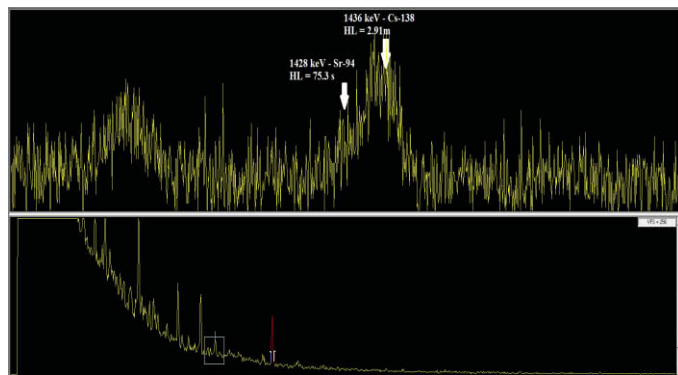

Fig. 3. A delayed gamma ray spectrum measured in the interlace mode showing peaks from Sr-94 and Cs-138.

B. Delayed Gamma Spectra Measured in between Linac Pulses

Interlace mode measurements described above are straight-forward and put less stress on the electronics and detectors. However, the majority of fission products have relatively short half-lives. After being produced during each linac pulse, these fission products quickly decay away. In interlace mode, for short-lived fission products, only the last few pulses would make contribution to the final spectrum. In order to capture short-lived isotopes and increase the sensitivity of the measurement, it is preferred that spectrometry measurements be performed in between linac pulses. Because of the huge energy deposition during each pulse, the detector and front-end electronics are saturated for a relatively long time period (~tens of ms). After this, the baseline slowly returns to zero, as shown in Fig. 4. Traditional shaping methods cannot handle this behavior very well, so the measurements have to be gated. In the following measurement, the linac was running at 20 Hz, i.e. the time interval between two adjacent pulses is 50 ms. After each pulse, the MCA waits for 20 ms before starting processing incoming signal. The counting continues for 20 ms before the MCA is disabled right before the next pulse arrives.

Using this method, delayed gamma spectra were measured with both a DU sample and a HEU sample, as shown in Fig. 5. Peaks from fission products (e.g. Sr-94 and Cs-138) are clearly observable, despite the fact that our counting time was quite limited (~ 500 s with at least 50% dead time). Because of the

poor counting statistics and the low detector efficiency at higher energies, we were not able to quantitatively study the difference between HEU and DU spectra. The degradation in energy resolution caused overlapping between gamma peaks from the check source and fission products, which makes it even harder to analytically report the measurement results.
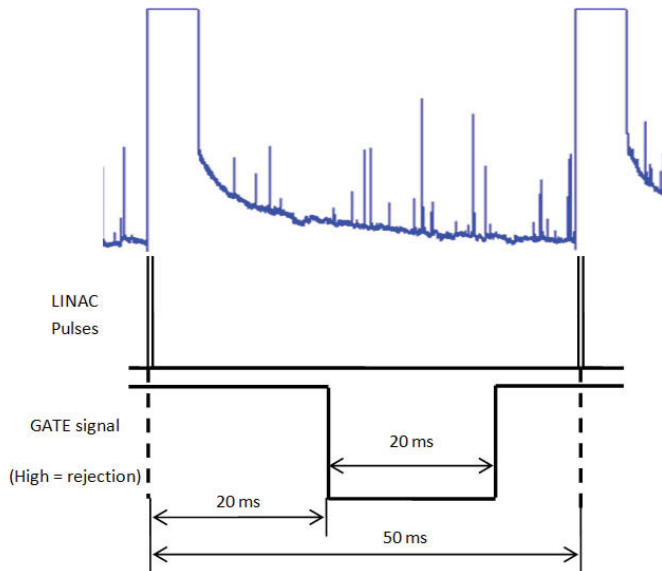

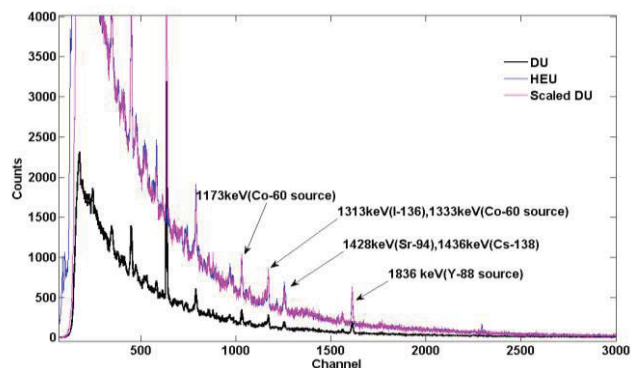Fig. 4. The output signal from the pre-amplifier when the linac beam is on.

Fig. 5. Delayed gamma ray spectra measured with a DU sample and a HEU sample.

III. MONTE CARLO SIMULATION OF DELAYED GAMMA RAYS

This portion of our investigation aims to accurately simulate gamma-ray distributions from photon induced fission reactions using the MCNP5/MCNPX Monte Carlo simulation platform. These simulations are used to model experimental conditions, including target and shielding materials, the detector, and the linac, which then allows us to predict and optimize experimental parameters. Recent collaboration at Idaho Accelerator Center (IAC) has enabled the collection of experimental photofission data to be used for benchmark comparisons with our MCNP numerical models.

In order to accurately obtain delayed gamma signatures using MCNPX, the software's photofission library must first

be initialized to ensure the coincidence counting of photofission particles. By enabling the analog production of photons from photofission reactions, specific isotopes identified from the ENDF/B-VII photonuclear data library are used for the simulation of photonuclear particle production. Photonuclear reactions within MCNPX are controlled using the software's Photon Physics Options within the PHYS:P card. Tally cards specifying photon flux, energy and time, were used for the parameterization of each calculated photofission distribution. Within the code, the F4 flux tally averages the number of scored particles per area, and is set to do so within designated time and energy bins. The tally energy card, E4, defined the upper and lower bounds for particle energies on the order of ~3MeV at the time of scoring. The specific time intervals expected for delayed emissions were set using the tally time card T4. The counting of short-lived fission products following linac pulses performed experimentally are accurately modeled using the variability of these tally cards. Photon flux distributions are used to model expected gamma-ray spectra for a variety of target materials. Analysis of each spectrum allows identification of specific energy peaks also expected for each photofission reaction. Simulations involving these delayed signatures were performed for a number of isotopes including Pu-239 and a number of mixed U-235/U-238 compositions. The normalized photon flux as a function of energy for the photofission reaction of a U-235/U-238 mixture is plotted below.
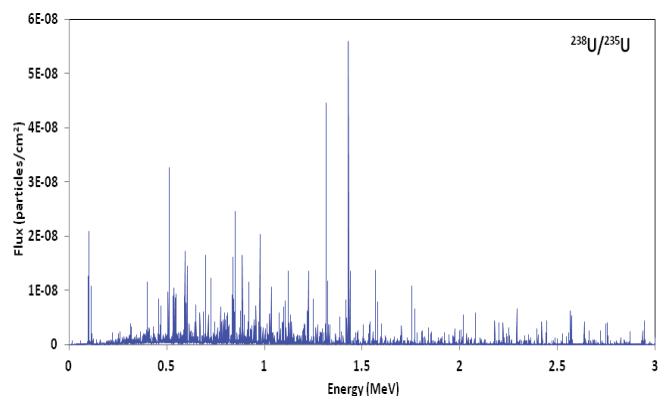

Fig. 6. An MCNPX simulation of the delayed gamma rays emission spectrum from a U-235 and U-238 mixture.

Identification and assessment of numerical photofission yields also provide information used to solve for isotopic concentration in target materials. Spectra for pure samples of U-238 and U-235 were modeled to form basis spectra used to de-convolve mixed U-235/U-238 samples as shown in Figure 6. The overlapped energy spectra for pure uranium samples shown in Figure 7 are indicative of sum peak contributions for each uranium mixture.

The sum of these energy peaks at 974.6 keV, 1.31 and 1.43 MeV are used to determine the isotopic composition for both U-238 and U-235 fissionable isotopes. The summation of peak

ratios in each pure sample is then set equal to the peak ratio of the mixture. Repeating this step for two additional energy peaks, allows for the formation of a set of two equations with two unknowns. For example, using the three energy peaks indicated in Figure 7, the following equations are solved to find the U-238/U-235 concentrations within this mixture:

$$\left(\frac{peak\ 1}{peak\ 2}\right)_{mixture} = C_1\left(\frac{peak\ 1}{peak\ 2}\right)_{238} + C_2\left(\frac{peak\ 1}{peak\ 2}\right)_{235}$$

$$\left(\frac{peak\ 1}{peak\ 3}\right)_{mixture} = C_1\left(\frac{peak\ 1}{peak\ 3}\right)_{238} + C_2\left(\frac{peak\ 1}{peak\ 3}\right)_{235}$$

Where the coefficients C1 and C2 indicate the quantity of each pure uranium isotope within the mixture. These equations can then be solved given the known values of each energy peak. Analysis of the U-238 concentration in this example yielded 91.3%, differing by 1.7% from the known concentration. Although this method of isotopic analysis has proven useful in this approximation, uncertainties within the MCNPX simulations still exist. These uncertainties may result from deficiencies in the number of scored particles during Monte Carlo calculations. The spectra discussed here and others alike are designated to run 10^6 source particles during calculation. At this time, immediate development of calculations involving increased particle counts on the order of 10^9 is underway in an effort to resolve counting uncertainty.
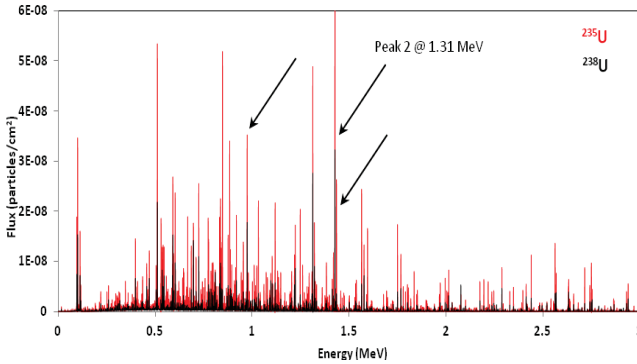

Fig. 7. MCNPX simulation of the delayed gamma rays emission spectrum from a pure U-235 sample and a pure U-238 sample.

Recent tests run at IAC focused primarily on photofission measurements involving Pu-239, Th-232, and Depleted Uranium (DU) plates. Run time data acquisition provided accurate benchmark spectra which were referenced using our teams MCNP simulations. Although our team was equipped with calculated spectra for Pu-239 and U-235/U-238 mixtures, limitations due to available photonuclear data libraries in MCNPX restricted simulation of Th-232.

IV. DIGITAL SIGNAL PROCESSING TECHNIQUES

High throughput spectroscopy systems are being investigated. A major challenge in the proposed work is to perform high energy resolution gamma spectroscopy at an ultra-high throughput rate with good accuracy. The HPGe detector is the only practical candidate that can provide excellent energy resolution in a wide energy range as needed in measurements of delayed gamma spectroscopy. Innovative spectroscopy systems are being developed using advanced signal processing techniques to improve the throughput rate of HPGe detectors without sacrificing energy resolution. Real-time digital signal processing methods will then be implemented and tested. Previous study showed that digital filtering can greatly improve throughput rate with little degradation in energy resolution [22]. Various filters are currently being evaluated in this work, e.g. moving window de-convolution (MWD) and the trapezoidal filters. Recent study showed great potential of the template-matching method in high rate applications [24]. Instead of filtering the energy signal, a pre-defined pulse shape template is used in this method to de-convolve the signal train. This method will be further evaluated.

As a start, a LABVIEW interface has been developed to enable streaming of digitized data to the hard drive at full speed (100 MSPS, 14-bit) if one channel is utilized, or at half of the full speed (50 MSPS, 14-bit) if both channels on the digitizer are utilized. The speed of data streaming is mainly limited by the write speed of the hard drive. In our case, two Intel Solid State Disks are configured in RAID 0 array to maximize the transfer rate. The LABVIEW interface is shown below in Fig. 8.
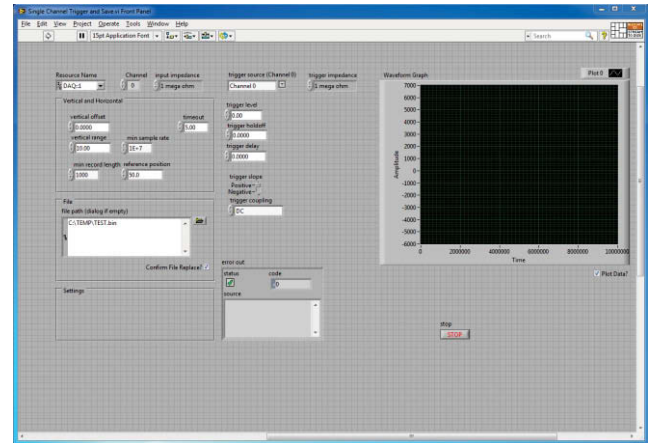

Fig. 8. User interface of the LABVIEW data acquisition program.

Using this interface, we were able to configure and control the digitizer. In the initial test, the digitizer is triggered by the linac pulses. During the measurements, the linac was running at 10 Hz, i.e. the time interval between two adjacent pulses is 100 ms. The digitizer is configured to record data for 120 ms each time it is triggered.

As can be observed from Figure 4, the detector output is saturated for roughly 10 ms in this particular case. The recovery time is related to the energy deposition in the detector (i.e. beam current, beam energy, shielding around the detector, detector volume, target in the beam, etc.). After each linac pulse the baseline of the detectors output signal slowly returns

to normal after about 40 ms. Therefore, for linac operations at 10 Hz provides the detector about 50 ms of data at the baseline per pulse. Efforts have been made to improve the DSP algorithms for high throughput applications. DSP algorithms based on trapezoidal filters are being developed and evaluated. A trapezoidal shaper can be implemented as shown below in Fig. 9.
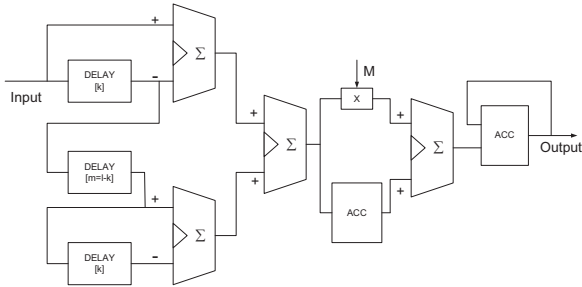

Fig. 9. Implementation of a trapezoidal filter.

To implement pile-up rejection, two channels are designed. The output signal from the pre-amplifier are passed through these two channels in a parallel manner: a fast channel for timing and a slow channel for energy information. The figure below shows the original signal (blue) and the outputs from the fast (red) and slow channel (black).
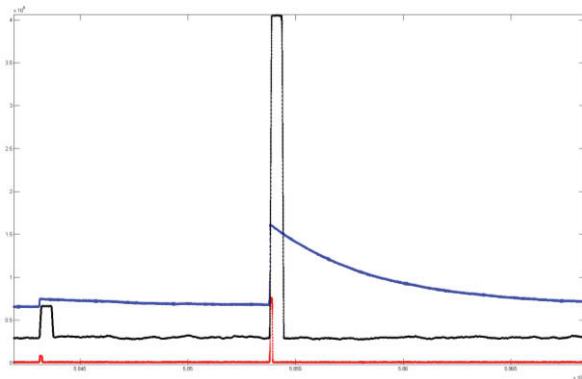

Fig. 10. Digital signal processing using a trapezoidal filter.

Improvements have been implemented on the shaping algorithm. Instead of using an overall estimation, the baseline of the output signal is measured right before the rising edge of each pulse. By doing this, the energy degradation due to drifting of baseline can be minimized. Using typical values for rising edge and flat top, an energy spectrum was achieved as shown in Fig. 11.

For comparison purposes the digitized data shown in Figure 11 is plotted with the same energy spectrum measured with a commercially available MCA, Canberra LYNX system (data with red dots), is displayed in Figure 12. It can be observed that the energy resolution achieved using the customized DSP algorithm based on trapezoidal filters is very comparable to the results obtained using commercially available software.

The next step in this work is to optimize this customized DSP algorithm for high-throughput applications.
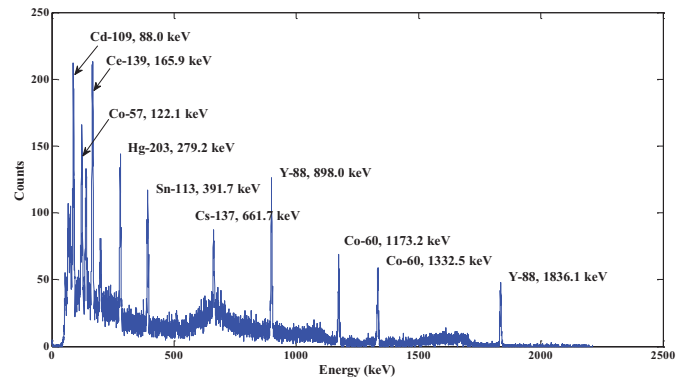

Fig. 11. An energy spectrum reconstructed using digitized data via a trapezoidal filter.
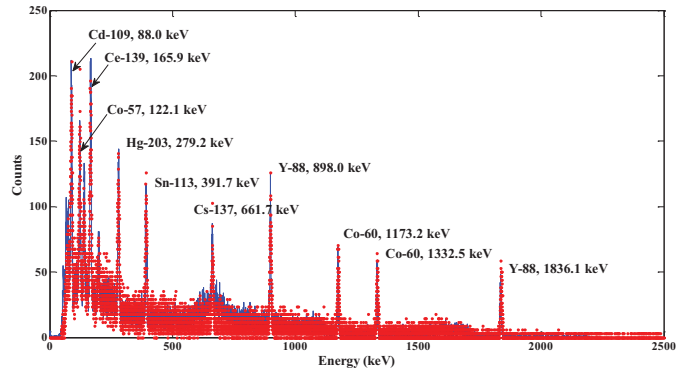

Fig. 12. Comparison between energy spectra obtained using a commercially available MCA and the signal processing unit developed in this work.

V. CONCLUSIONS AND FUTURE WORK

Active interrogation techniques based on delayed gamma rays emitted by photofission products are being developed for nuclear safeguards applications. The ultimate goal is to directly measure Pu-239 content in nuclear spent fuel. The results from an initial testing were discussed. Energy spectra of delayed gamma rays were measured in both interlace mode and in between linac pulses. A simulation platform is being developed using MCNPX simulation package. To address the ultra-high throughput rate need for spent fuel measurements, spectrometry systems based on digital signal processing technology is under investigation. Currently, the shaping algorithm is limited to trapezoidal shaping. Other algorithms are to be implemented and evaluated.

REFERENCES

[1]   J. L. Jones, et al., Photofission-based, nuclear material detection: technology demonstration, INL Report 02-01406, December 2002.

[2]   J. L. Jones, et al., Pulsed photonuclear assessment (PPA) technique: CY04 year-end progress report, INL Report 05-02583, February 2005.

[3]   J. L. Jones, et al., Photonuclear-based, nuclear material detection system for cargo containers, *Nucl. Instr. and Meth. B* 241 (2005) 770.

[4]   D.R. Norman, et al., Inspection applications with higher electron beam energies, *Nucl. Instr. and Meth. B* 241 (2005) 787.

[5]   J. L. Jones, et al., Detection of shielded nuclear material in a cargo container, *Nucl. Instr. and Meth. A* 562 (2006) 1085.

[6]   D. R. Norman, et al., Time-dependent delayed signatures from energetic photon interrogations, *Nucl. Instr. and Meth. B* 261 (2007) 316.

[7]   C. L. Hollas, et al., Analysis of fissionable material using delayed gamma rays from photofission, LA-UR-06-3363, 1986

[8]   C. L. Hollas, et al., Analysis of fissionable material using delayed gamma rays from photofission, *Nucl. Instr. and Meth. B* 24 (1987) 503.

[9]   D. H. Beddingfield, et al., Identification of fissile materials from fission product gamma-ray spectra, *Nucl. Instr. and Meth. A* 417 (1998) 405.

[10] M. Gmar, et al., Use of delayed gamma spectra for detection of actinides (U, Pu) by photofission, *Nucl. Instr. and Meth. A* 422 (1999) 841.

[11] F. Carrel, et al., Identification of actinides inside nuclear waste packages by measurement of fission delayed gammas, *IEEE Nuclear Science Symposium Conference Record, pp. 909-913*, 2006

[12] F. Carrel, et al., Identification and differentiation of actinides inside nuclear waste packages by measurement of delayed gammas, *IEEE Trans. Nucl. Sci., Vol. 57*, pp. 2862, 2010

[13] M. T. Kinlaw, et al., Fissionable isotope identification using the time dependence of delayed neutron emission, *Nucl. Instr. and Meth. A* 562 (2006) 1081.

[14] E. T. E. Reedy, et al., The detection of delayed gamma-rays between intense bremsstrahlung pulses from discriminating fissionable from non-fissionable materials, *Nucl. Instr. and Meth. A* 60 (2009) 811.

[15] S. Kahane, et al., Photofission of U-238 with neutron-capture gamma rays, *Phys. Rev. C 32*, 1944-1955 (1985)

[16] D. Dore, et al., Delayed neutron yields and spectra from photofission of actinides with bremsstrahlung photons below 20 MeV, *J. Phys.: Conf. Ser.* 41, 241

[17] R. B. Walton, et al., Delayed Gamma Rays from Photofission of U-238, U-235, and Th-232, *Phys. Rev. 134*, B824–B832 (1964)

[18] M. Gmar, et al., Assessment of actinide mass embedded in large concrete waste packages by photon interrogation and photofission, *Appl. Radiat. Isot., Vol. 63, pp. 613*, 2005

[19] K. Baumung, K. Bohnel, J. Klunker, M. Kuchle, and J. Wolff, "Investigations into nondestructive safeguards techniques," Proceedings IAEA-Karlsruhe, Germany Symposium on Safeguards Techniques, vol. 2, pp. 192, 1970

[20] General Atomics, Application of photo induced reactions to nuclear materials safeguards problems, GA-9614, San Diego, California, 1969

[21] D. Wehe, et al., Observation of [238]U photofission products, *IEEE Trans. Nucl. Sci., Vol.* 53, no. 3, pp. 1430, 2006

[22] H. Yang, et al., Spectroscopy of high rate events during active interrogation, *Nucl. Instr. and Meth. A* 598 (2009) 779.

[23]   D. Norman, et al., Methods Relating to Photonuclear Detection, Patent Application Publication, Pub. No. US 2012/0082282 A1, 2012

[24] P. Scoullar, et al., High count rate low dead time digital pulse processing utilizing real time pulse pile-up recovery, *IEEE Nuclear Science Symposium*, 2010